International Journal of Information, Control and Computer Sciences
ISSN: 2517-9942
Vol:5, No:11, 2011

# Modeling and Control of Direct Driven PMSG for Ultra Large Wind Turbines

Ahmed M. Hemeida, Wael A. Farag, and Osama A. Mahgoub

***Abstract*—**This paper focuses on developing an integrated reliable and sophisticated model for ultra large wind turbines And to study the performance and analysis of vector control on large wind turbines. With the advance of power electronics technology, direct driven multi-pole radial flux PMSG (Permanent Magnet Synchronous Generator) has proven to be a good choice for wind turbines manufacturers. To study the wind energy conversion systems, it is important to develop a wind turbine simulator that is able to produce realistic and validated conditions that occur in real ultra MW wind turbines. Three different packages are used to simulate this model, namely, Turbsim, FAST and Simulink. Turbsim is a Full field wind simulator developed by National Renewable Energy Laboratory (NREL). The wind turbine mechanical parts are modeled by FAST (Fatigue, Aerodynamics, Structures and Turbulence) code which is also developed by NREL. Simulink is used to model the PMSG, full scale back to back IGBT converters, and the grid.

***Keywords*—**FAST, Permanent Magnet Synchronous Generator (PMSG), TurbSim, Vector Control and Pitch Control

## I. Introduction

WIND is a promising source of energy. In worldwide there are now many thousands of wind turbines operating, with a total nameplate capacity of 196,630MW [1]. There are many configurations of generating schemes in wind turbines. The two most interesting configurations are DFIG (Doubly Fed Induction Generator) with partially 30% back to back converters and the direct driven PMSG with full scale power converters. Many papers [2; 3] have proven that the direct driven PMSG is a good choice due to the elimination of gearbox, the advances in power electronics technology, the higher efficiency of PMSG and the wide range of speed control in the PMSG.The full scale power converters are divided into generator and grid side converters. The generator side converter is used mainly to control the electrical torque of the generator to obtain the optimum power. The grid side converter is used mainly to control the dc bus voltage and the reactive power flow to the grid. In this paper vector control is used to control the two converters.The work in this paper can be divided into three parts. The first part focuses in modeling of each part of the system starting with the wind simulator, the wind turbine, the generator, the converters and ending with the grid. Second part explains the control of each part of this system. The third part discusses the simulation results.

Ahmed M. Hemeida, teaching assistant with Cairo University, Faculty of Engineering, Electrical Power and Machines department; (e-mail: a.hemeida@live.com).
Wael A. Farag , Assistant Professor with Cairo University, Faculty of Engineering, Electrical Power and Machines department; (e-mail: wafarag@gmail.com).
Osama A. Mahgoub, Profeesor with Cairo University, Faculty of Engineering, Electrical Power and Machines department; (e-mail: mahgoub04@yahoo.com). .

## II. Modeling And Description Of The System

The model of the system will be explained in this section. The main parts shown in Fig. 1 which are described in next section are: (1) stochastic wind flow generated by Turbsim, (2) FAST nonlinear wind turbine model, (3) the direct driven PMSG, (4) AC-DC-AC converter, and (5) the grid model.

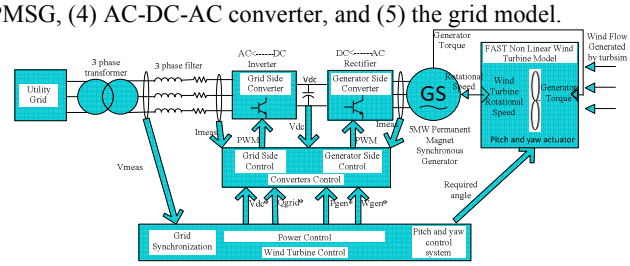

Fig. 1 Block diagram of wind turbine system

### A. Turbsim for Simulation of Wind

Turbsim is a stochastic, full field wind simulator. It uses statistical model to numerically simulate time series of three wind components in a dimensional grid. It is used to be an input to FAST program to provide it with the required wind field data. Spectra of velocity components and spatial coherence are defined in the frequency domain, and an inverse Fourier transform produces time series [4].

Its purpose is to provide the wind turbine designer with the ability to drive design code simulations of advanced turbine designs with simulated inflow turbulence environments that incorporate many of the important fluid dynamic features known to affect turbine aero elastic response and loading [5].

### B. FAST Wind Turbine Model

The FAST (Fatigue, Aerodynamics, Structures and Turbulence) shown in Fig. 2 is capable of predicting both the extreme and fatigue loads of two-and three-bladed horizontal-axis wind turbines. It is proven that the structural model of FAST is of higher validity than other codes. During time-marching analysis, the FAST makes it possible to control the turbine [5; 6].

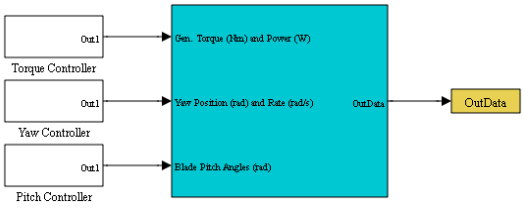

Fig. 2 FAST nonlinear wind turbine model in Simulink

FAST model gives the accessibility to control the generator torque, the pitch angle, the yaw angle of the nacelle, the high speed shaft (HSS) brake and deploying the tip brakes. All these controllers can be implemented in Simulink.

An interface has also been developed between FAST and Simulink with Matlab enabling users to implement advanced controls in Simulink convenient block diagram form. The FAST subroutines have been linked with a Matlab standard gateway subroutine in order to use the FAST equations of motion in an S-Function that can be incorporated in a Simulink model [7].

The wind turbine block, as shown in Fig. 3, contains the S-Function block with the FAST motion equations. It also contains blocks that integrate the degree of freedom accelerations to get velocities and displacements [7].

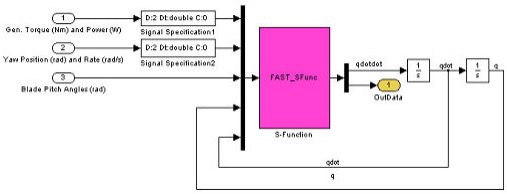


Fig. 3 FAST wind turbine S-function

To support concept studies aimed at assessing large wind technology, NREL developed the specifications of a representative utility-scale multimegawatt turbine now known as the "NREL offshore 5-MW baseline wind turbine" [6] which is dedicated for the 5MW wind turbine. This wind turbine is a conventional three-bladed upwind variable-speed variable blade-pitch-to-feather-controlled turbine. To create the model, they obtained some broad design information from the published documents of turbine manufacturers, with a heavy emphasis on the REpower 5MW machine.

The specifications of the 5MW wind turbine is shown in Appendix [6].

The output power of wind turbine can be defined as the difference between the power in the moving air before and after the rotor [8];

$$P_{wt} = \frac{1}{2}\rho\pi R^2 V_w^3 C_p(\lambda,\beta) \quad (1)$$

where ρ represents the air density, $V_w$ represents the wind speed, R represents the blade radius, and $C_p$ represents the power coefficient. The maximum value of $C_p$ is between 0.4 and 0.5 which is less than Betz's limit 0.59. The value of $C_p$ is function of tip speed ratio λ and pitch angle β.

$$\lambda = \frac{\omega * R}{V_w} \quad (2)$$

where $\omega_m$ is the rotational speed (rad/sec).

The rotor torque can be expressed as;

$$T_{wt} = \frac{\frac{1}{2}\rho\pi R^2 V_w^3 C_p(\lambda,\beta)}{\omega_m} \quad (3)$$

and the electro mechanical equation of the system can be expressed as:

$$T_{wt} - T_e = J\frac{d\omega}{dt} \quad (4)$$

where $T_e$ the electromagnetic torque of the generator and J is the inertia of the system.

*C. 5MW Direct Driven PMSG Modeling*

*1) Machine Equivalent Model*

Before obtaining the equivalent model of the radial flux PMSG in Fig. 4, it is necessary to calculate the total number of poles and introduce constraints on the leakage ratio of the machine. The equivalent model will then be derived in terms of number of stator conductors, $N_s$ based on the physical construction of the machine described in [9], yielding the induced voltage, $E_{pm}$, the synchronous inductance, $L_s$, and the stator resistance, $R_s$ from equations described in [10; 14]. Finally, parameters and machine equations are transposed in the rotor reference frame. This is more illustrated in [9; 10; 11].

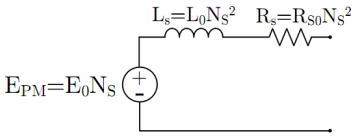


Fig. 4 Electrical diagram in terms of $N_s$

The data for the PMSG is shown in Appendix.

*2) General Equations*

The back e.m.f $Epm_{ln}^{max}$ produced by the magnets depends on the mechanical rotational speed $\omega_m$(rad/sec). This is illustrated in the following equations;

$$Epm_{\ln}^{\max} = \omega_e * \varphi_{pm} \quad (5)$$

where $\omega_e$ is the electrical rotational speed (rad/sec) and $\phi_{pm}$ is the flux linkage established by magnets (V.S).

$$\omega_e = P * \omega_m \quad (6)$$

where P = number of pole pairs.

*3) Dqo Equations*

Almost all drive systems use the dynamic dqo model of a machine. This converts the 3 phase ac quantities to dc quantities, which can be easily controlled by a simple proptional integral (PI) controller. The transformation from 3 phase variables with time varying (abc) frame to stationary dq0-frame defined in Fig. 5 [12].

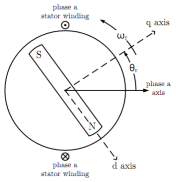


Fig. 5 Synchronization for the rotor position for the park transformation

Machine equations based on the rotor reference position are described in Equations (7) and (8) and they are marked with the subscript "r".

$$V_q^r = -R_s I_q^r - L_q\frac{dI_q^r}{dt} - \omega_r L_d I_d^r + \omega_r \varphi_{pm} \quad (7)$$

$$V_d^r = -R_s I_d^r - L_d\frac{dI_d^r}{dt} + \omega_r L_q I_q^r \quad (8)$$

The Variables $R_s$, $L_d$ and $L_q$ are the stator resistance, direct and quadrature inductance respectively of permanent magnet synchronous generator, where $L_d = L_q = L_s$.

Fig. 6 shows the equivalent circuit of the PMSG in d-q axis. The electrical torque is shown in equation (9). It is clear that to control the electrical torque the q-axis current can be controlled.

$$T_e = \frac{3}{2} P \varphi_{pm} I_q^r \tag{9}$$

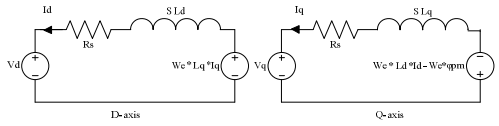


Fig. 6 Equivalent circuit of PMSG in d-q reference frame

*D. Converter Model*

The back-to-back converter is composed by a force-commutated rectifier and a force-commutated inverter as shown in Fig. 7 each is composed of six insulated gate bipolar transistor (IGBT) connected with a common DC-link.

An advantage of this system is the dc link capacitor which decouples the two converters and a separate control on each converter can be used.

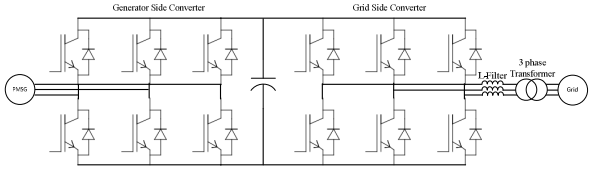


Fig. 7 Structure of the back to back voltage source converter (VSC)

A drawback of this system is the increase of the switching losses and also the presence of the DC-Link capacitor since it is bulky and heavy. It increases the cost and may be of most importance. This reduces the overall life time of the system [13]. The equivalent circuit of a voltage source converter is shown in Fig. 8.

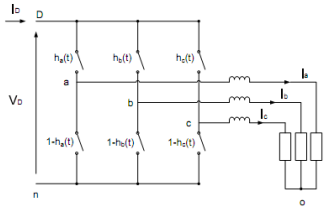


Fig. 8 Equivalent circuit of voltage source converter with ideal switch

The DC current $I_{dc}$ is expressed as;

$$I_{dc} = (h_a(t) I_a + h_b(t) I_b + h_c(t) I_c) \tag{10}$$

where $h_a(t)$, $h_b(t)$ and $h_c(t)$ are the switching status of the switches in VSC.

The output phase voltages are expressed by the following equation, which are dependent on $h_a(t)$, $h_b(t)$ and $h_c(t)$.

$$\begin{bmatrix} V_{an} \\ V_{bn} \\ V_{cn} \end{bmatrix} = \frac{V_{dc}}{3} \begin{bmatrix} 2 & -1 & -1 \\ -1 & 2 & -1 \\ -1 & -1 & 2 \end{bmatrix} \begin{bmatrix} h_a(t) \\ h_b(t) \\ hc(t) \end{bmatrix} \tag{11}$$

This topology is used for full rating power converter in some large scale wind turbines [14; 15].

*E. Grid Model*

The grid can be represented as shown in Fig. 9. The output of the coupling is represented by subscript U and grid voltage is represented by subscript E.

The voltage equation per phase can be described as follows:

$$E = U + R_s * I + L_s * \frac{dI}{dt} \tag{12}$$

where $R_s$ and $L_s$ represent the equivalent series resistance and inductor of the filter and transformer between grid and inverter output.

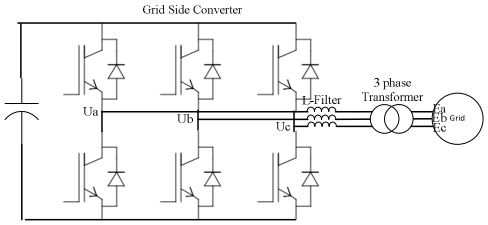


Fig. 9 Grid Side Converter

For a three phase voltages with a rotating frame angle Θ which starts rotating with phase a, the amplitude of the phase voltages of the grid ($E_{an}$, $E_{bn}$, $E_{cn}$) which equals $E_s$ will be placed on the d- axis ($E_d = E_s$). The q-axis component voltage will be zero. Then converting Equation (12) to d-q frame results in the following equations;

$$V_q^r = R_s I_q^r + L_q \frac{dI_q^r}{dt} + \omega_r L_d I_d^r + 0 \tag{13}$$

$$V_d^r = R_s I_d^r + L_d \frac{dI_d^r}{dt} - \omega_r L_q I_q^r + E_s \tag{14}$$

where $V_d^r$ and $V_q^r$ are the d-q output voltages of the inverter, $\omega_r$ is the grid frequency in rad/sec, $L_d$ and $L_q$ are the inductance in d-q axis which equal $L_s L_s$ and $I_d^r$ and $I_q^r$ are the d-q axis currents.

The equations of active and reactive power converted to grid are shown in Equations (15), (16). It's shown that to control active power the d-axis current must be controlled and to control reactive power the q-axis current is needed to be controlled as shown in the following equations.

$$P = \frac{3}{2} E_s * I_d \tag{15}$$

$$Q = \frac{3}{2} E_s * I_q \tag{16}$$

The data for the grid configuration is shown in Appendix.

## III. Control of PMSG based Wind Turbines

The requirements of any turbine control system are to extract almost all the output power of the wind turbine. Four regions can be defined for the control of the wind turbine as shown in Fig. 10.

- In region 1, the output power from the wind turbine is too low, this won't be sufficient to operate the wind turbine.
- Region 1.5 is a linear transition between regions 1 and 2. This starts from 6.9 rpm and ends at 30% above the starting rotor speed.

➢ In region 2, the controller is adjusted to extract almost all the output power available in the wind turbine. This is done by changing the electromagnetic torque of the generator to always work on maximum power coefficient. This region ends at 99% of the rated rotor speed. This is done by the generator side converter and this is more illustrated in Section III.A.

➢ Region 2.5 is a linear transition between regions 2 and 3. This region is required to limit tip speed at rated power. This region ends at rated rotor speed.

➢ In region 3, the generator electromagnetic torque is kept constant and the pitch angle is adjusted to keep the rotor speed constant at its nominal value. Therefore, the output power is kept constant.

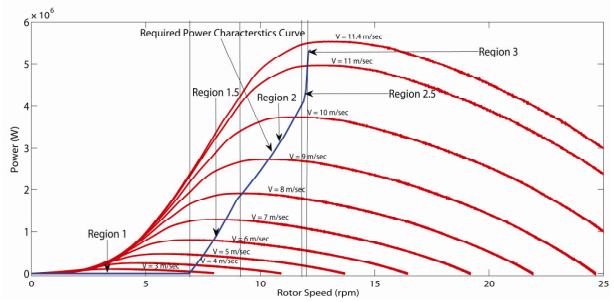


Fig. 10 Power curve for wind turbine

### A. Generator Side Converter Control

Type of control used is field oriented control (FOC) as shown in

Fig. 11. This type of control gives high performance. FOC uses the shaft speed, obtained by an encoder as a feedback in the control strategy.

The d and q axis current component represents the components of flux and torque. The torque and flux can be controlled separately for the current control loops.

Constant Torque Angle Control (CTA) is the control technique used to control the d and q axis currents. CTA keeps the torque angle constant (angle between the stator current vector and the rotor permanent magnet flux) at 90°. This is done by keeping the stator current reference in d-axis at zero, to produce maximum torque per ampere; therefore the resistive losses are minimized. The stator current reference in q-axis is calculated from the reference torque using Equation (9) [16].

The required d-q components of the voltage vector are derived from two PI current controllers. After the PI current controllers, compensation terms in the following two equations are added to improve the transient response. They are obtained from Equations (7) and (8).

$$Component \rightarrow 1 = \omega_r L_q I_q^r \tag{17}$$

$$Component \rightarrow 2 = -\omega_r L_d I_d^r + \omega_r * \varphi_{pm} \tag{18}$$

Space Vector Modulation (SVM) is the technique used to create the duty cycles of the desired reference voltages. The PWM switching signals for the power converter switching devices can be obtained by comparing the duty cycles with the carrier signal in order to create. The PI parameters are designed using sisotool in MATLAB as described in [17].

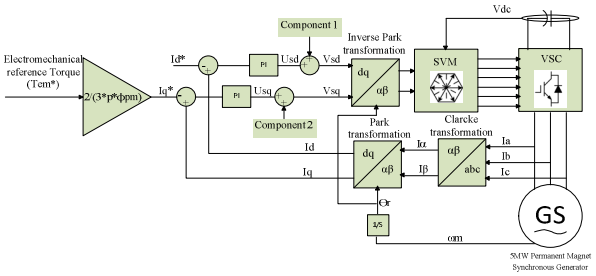


Fig. 11 Generator Side Control

The reference of the electromagnetic torque $T_{em}^*$ can be calculated by using optimal torque control method [18]. This control method uses the measured rotational speed (rad/sec) of the shaft and the parameters of the wind turbine to obtain the optimal operating point. The output wind turbine power is obtained from Equation (3).

$$P_{wt} = \frac{1}{2}\rho\pi R^2 V_w^3 C_p(\lambda,\beta) = \frac{1}{2}\frac{C_p(\lambda,\beta)}{\lambda^3}\rho\pi R^5 \omega_m^3 \tag{19}$$

By replacing $\lambda(t)$ by $\lambda_{opt}$ and $C_p(\lambda,\beta) = C_p(\lambda_{opt},\beta)$, the reference power can be obtained in region 2.

$$P_{wt_{opt}} = K\omega_m^3 \tag{20}$$

where;

$$K = \frac{1}{2}\frac{C_p(\lambda,\beta)}{\lambda^3}\rho\pi R^5 \qquad N.m/(\frac{rad}{\sec})^2 \tag{21}$$

The reference torque is calculated as follows;

$$T_{wt_{opt}} = K\omega_m^2 \tag{22}$$

The value of K for the 5MW wind turbine system is 23342.87N.m/rpm$^2$.

### B. Pitch Angle Control

The basic aim of pitch control scheme is to keep constant rated power at region 3. Blade pitch actuator for the 5MW wind turbine has a maximum rate limit of 8 degree/sec. Also, the minimum and maximum blade pitch settings are 0° and 90° respectively [6]. The blade pitch actuator is a second order system with a very high natural frequency of 30Hz and a damping ratio of 2% [6].

Fig. 12 shows the control scheme for pitch system. The rotational speed is kept constant at rated speed by increasing pitch angle. This will reduce the aerodynamic torque produced by the wind turbine. Below rated rotor speed the pitch angle is adjusted at its lower limit.

The PI gains are designed by linearizing the FAST model at wind speed of 18m/sec and by using sisotool in Matlab the gains are obtained.

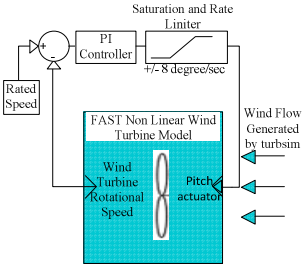


Fig. 12 Pitch Angle Control Scheme

### C. Grid Side Converter Control

The aim of the control as shown in Fig. 13 is to transfer all the active power produced by the wind turbine to the grid and also to produce no reactive power so that unity power factor is obtained, unless the grid operator requires reactive power compensation. In Fig. 13 the phase locked loop (PLL) is used to synchronize the three phase voltage with the grid voltage. The main aim of the controller is to:

- Regulate the DC bus voltage constant to be greater than the amplitude of the grid line to line voltage. This is done by controlling the d-axis current component. So, if turbine Power $P_t$ and generator power $P_g$ are equal, $V_{dc}$ must be constant.

$$I_c = C\frac{dV_{dc}}{dt} = \frac{P_t}{V_{dc}} - \frac{P_g}{V_{dc}} \quad (23)$$

where $I_c$ is the capacitor current.

- Control the reactive power through the q current component as can be concluded from Equation (16).

A compensation terms mentioned in the following equations, will be added to improve the transient response of the system which can be concluded from Equations (13) and (14).

$$Component \rightarrow 1 = -\omega_r L_q I_q^r + E_s \quad (24)$$

$$Component \rightarrow 2 = \omega_r L_d I_d^r \quad (25)$$

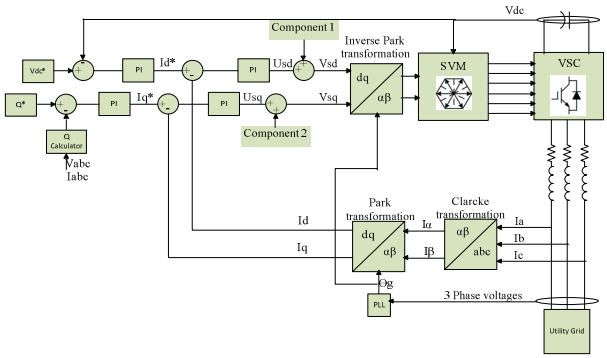


Fig. 13 Grid Side Converter Control

## IV. Simulation Results

The system is tested under two conditions. The first condition with the wind speed changes in steps. The pitch angle response for step changes for wind speed is shown in Fig. 14. The wind is changing from 12 to 20m/sec in 1m/sec steps. It is also observed that the rotor speed raises only 5% of the rated value. The power has an average value of 0.998p.u over the time period of 100sec. These values are within reasonable range.

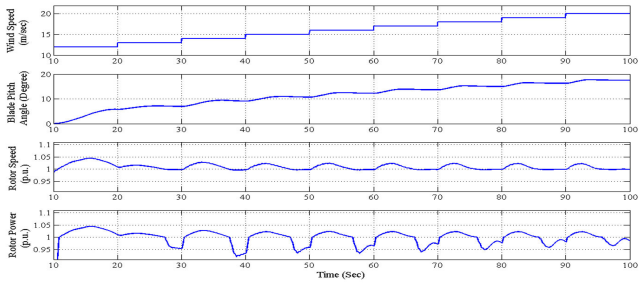


Fig. 14 Pitch angle response for step changes in wind speeds

Under the second condition a stochastic wind speed generated by Turbsim [4] will be used. The controller is tested with wind profile named great planes wind profile (GP_LLJ). This wind profile is standard, validated by IEC, and has a coherent structure. The hub height wind speed is shown in Fig. 15 with an average value of 18m/sec and a standard deviation of 1.15. It is shown that the rotor speed changes within 5% of the rated value. This value is within reasonable range. The power has an average value of 0.92p.u over the time period of 100sec.

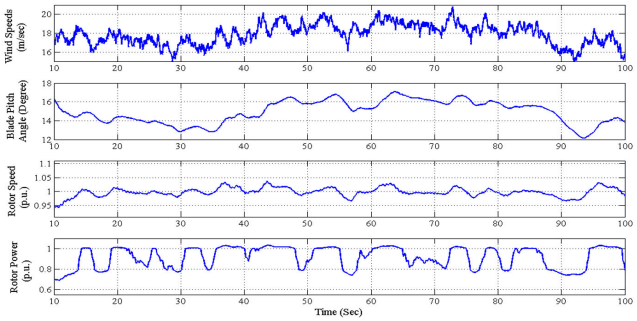


Fig. 15 Pitch angle response for stochastic wind speeds

### A. Generator and Grid Side Control

Two cases will be studied in this study. In the first case the generator and grid side controller are tested under wind speed steps of 2m/sec from 6 to 10m/sec as shown in Fig. 16.

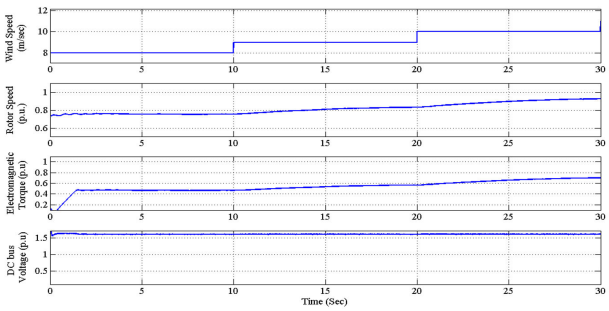


Fig. 16 Speed, electromagnetic torque and dc bus voltage response for wind speed variations

For every increase in wind speed the wind turbine aerodynamic torque increases and correspondingly the electromagnetic torque increases. The rotor speed also

increases and settles after duration of 5sec. This is due to the large inertia of the system. The dc bus voltage is set to be at 1.6p.u. It is also observed that the dc bus voltage isn't affected by the variations of wind speed. This is due to the electrical system response is very fast compared to the mechanical time constant.

Fig. 17 a and b show the d and q-axis responses for the generator currents. The generator d-axis current is set all over the simulation to zero to get the maximum torque/ampere and the q-axis is directly tracking the electromagnetic torque. The ripple is around 2%.

Fig. 17 c and d show the d and q-axis responses for the grid currents. The grid q-axis current is set all over the simulation to zero to get zero reactive power and the d-axis component is directly tracking the power flow from the turbine to the grid. The ripple in the d-axis current is around 4%. But in the case of the q-axis it increases to 10%.

Fig. 18 shows the phase a current of the grid for 10 cycles. It shows a THD of 3.76% which is quite acceptable.

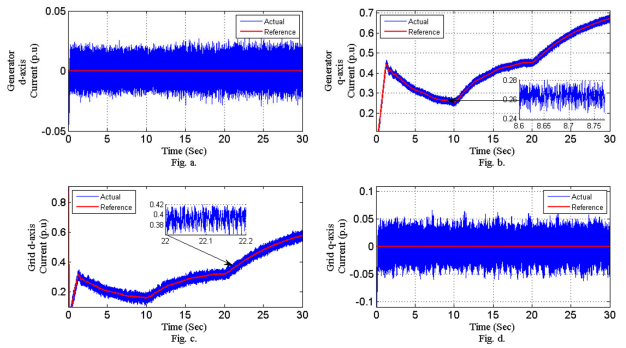


Fig. 17 D and Q axis currents response for generator and grid

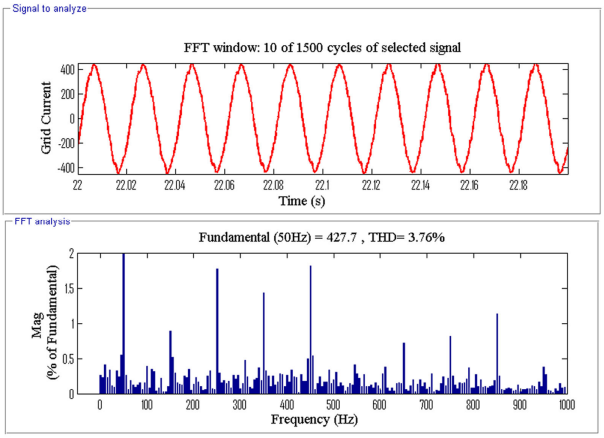


Fig. 18 Phase A Grid Current.

In the second case the controller is tested under turbulence wind which has a mean wind speed of 9.2m/sec, standard deviation of 0.381 and a power law exponent of 0.143 as shown in Fig. 19. The wind speed has stochastic wind variations. It varies about a mean value of 9m/sec. The rotor speed increases at first then it reaches a steady state value. Whenever the wind speed variations about the mean wind speed the system doesn't sense these variations due to the large inertia of the rotor. The generator is only affected by the mean wind speed.

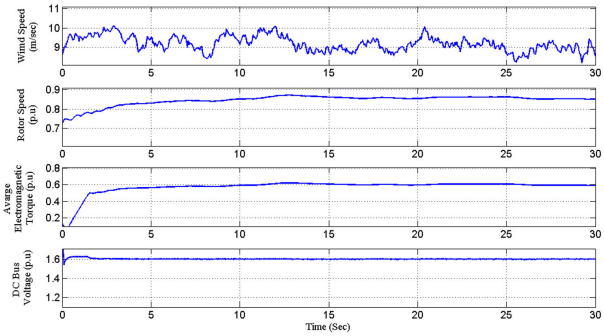


Fig. 19 Speed, electromagnetic torque and dc bus voltage response for wind speed variations

## V. Conclusion

The main objective of this paper was the modeling and simulation of the ultra large wind turbine system using validated models of wind turbine mechanical and electrical systems. Then the electrical system consisting of the generator, back to back VSC and the grid have been described mathematically component by component. Then the performance and analysis of vector control and the pitch control algorithms have been studied on the system. The simulation was conducted under conditions of step wind speeds and stochastic wind flow generated by TurbSim. The simulation results have shown the correct functioning of the controllers applied on each component in the whole system.

## Appendix

### Properties for the NREL 5-MW Baseline Wind Turbine

| Wind Turbine Parameters | |
|---|---|
| Rating | 5MW |
| Rotor Orientation, Configuration | Upwind, 3 Blades |
| Control | Variable Speed, Collective Pitch |
| Rotor and turbine inertia about the shaft | 38,759,228 $Kg.m^2$ |
| **Generator Parameters** | |
| Nominal Power $P_{gen,nom}$ | 5.3MW |
| Nominal Torque $T_{gen,nom}$ | 4.18MN.m |
| Generator inertia about the shaft | 5,025,500 $Kg.m^2$ |

Generator Side Characteristics

| Parameters | Value |
|---|---|
| No. of pair poles, P. | 100 |
| The r.m.s induced no load voltage at rated speed, $Epm_{ln}^{rms}$ . | 2.31KV |
| The stator resistance, $R_s$. | 0.08Ω |
| The magnetizing inductance, $L_{sm}$. | 3.352mH |
| The leakage inductance, $L_{sl}$. | 5.028mH |

Grid Side Characterstics

| Parameters | Value |
|---|---|
| Grid Voltage. | 4KV |

| | |
|---|---|
| Line filter inductance. | 4mH |
| DC bus voltage. | 6.4KV |
| DC bus capacitance. | 4000μF |

## ACKNOWLEDGMENT

This project has been funded by the Science and Technology Development Fund (STDF) project number 1411.

## REFERENCES

[1] Association, World Wind Energy. *World Wind Energy Report.* Cairo, Egypt : World Wind Energy Association WWEA 2011, 31 October.

[2] H. Polinder, F.F.A. van der Pijl, G.J. de Vilder, P. Tavner, *"Comparison of direct-drive and geared generator concepts for wind turbines", IEEE Trans. Energy Conversion, Vol. 21, pp. 725-733, September 2006.*

[3] D. Bang, H. Polinder, G. Shrestha, and J.A. Ferreira, *"Review of generator systems for direct-drive wind turbines", in Proc. EWEC (European Wind Energy Conference & Exhibition,) Brussels, Belgium, March 31 - April 3, 2008.*

[4] J. Jonkman, B.J. "*Turbsim user's guide".* s.l. : NREL/TP-500-46198: National Renewable Energy Laboratory., August 2009.

[5] Sayooj B Krishna, Reeba S V. *"Simulation Of Wind Turbine With Switched Reluctance Generator by FAST and Simulink".* .November 2009, National Conference on Technological Trends.

[6] J. Jonkman, S. Butterfield, W. Musial, and G. Scott. "*Definition of a 5-MW Reference Wind Turbine for Offshore System Development".* s.l. : NREL, February 2009.

[7] J. Jonkman, B.J. "*FAST User's Guide, Technical Report".* s.l. : NREL/EL-500-38230: National Renewable Energy Laboratory., August, 2005.

[8] Cristian Busca, Ana-Irina Stan, Tiberiu Stanciu and Daniel Ioan Stroe. *"Control of Permanent Magnet Synchronous of large wind turbines".* Denmark : Departament of Energy Technology: Aalborg University, November 2010, Industrial Electronics (ISIE), ieee, pp. 3871 - 3876 .

[9] D. Bang, H. Polinder, J.A. Ferreira. "*Design of Transverse Flux Permanent Magnet Machines for Large Direct-Drive Wind Turbines".* Electrical Power Processing / DUWIND, Delft University of Technology. Netherlands : Delft University of Technology, 2010. phD Thesis.

[10] Hui Li, Zhe Chen. "*Design Optimization and Evaluation of Different Wind Generator Systems".* February 2009, Sustainable Power Generation and Supply, 2009. SUPERGEN '09.

[11] Li, Hui, Chen, Zhe and Polinder, H. "*Optimization of multibrid permanent-magnet wind generator systems".* Security & New Technol., Chongqing Univ : IEEE Transactions on Energy conversion, March 2009, IEEE Transactions on Energy conversion , Vol. 24, pp. 82-92.

[12] P. C. Krause, O. Wasynczuk, and S. D. Sudho. "*Analysis of Electric Machinery and Drive System"s.* s.l. : John Wiley & Sons, , 2002.

[13] Floren lov, FredeBlaabjerg. "*Power electronics Control of wind energy in distributed power systems".* Department of energy technology, Aaloborg university. 2009. pp. 1–16.

[14] Shuhui Li, Timothy A.Haskew, Ling Xu. *"Conventional and novel control designs for direct driven PMSG wind turbines".* 3, March 2010, Electric Power Systems Research, Vol. 80, pp. 328-338.

[15] Remus Teodorescu, Pedro Rodriguez. "*Thesis in Reactive power control for wind power plant with STATCOM".* Institute of Energy Technology-Pontoppidanstræde 101. 2010. Master thesis.

[16] Busca, C., et al., et al. *"Vector control of PMSG for wind turbine applications".* s.l. : Dept. of Energy Technol., Aalborg Univ., Aalborg, Denmark , 2010 , Industrial Electronics (ISIE), pp. 3871 - 3876 .

[17] Andreea Cimpoeru, Kaiyuan Lu. "*Encoderless Vector Control of PMSG for wind turbine applications".* Institute of Energy Technology, Institute of energy technology. s.l. : AALBORG University, 2010. Master Thesis.

[18] Michael J. Grimble, Professor Michael A. Johnson. "*Optimal Control of Wind Energy Conversion Systems".* August 2007 .